Electronic structure of a many-electron spherical quantum dot with an impurity

Mehmet Şahin*
Faculty of Science and Arts, Physics Department, Selçuk University, Kampus 42031 Konya, Turkey

Mehmet Tomak
Physics Department, Middle East Technical University, İnönü Bulvari 06531 Ankara, Turkey
(Received 12 May 2005; published 15 September 2005; publisher error corrected 20 September 2005)

We investigate the electronic structure of a many-electron spherical quantum dot with and without hydrogenic impurity. The number of electrons is taken as $N=18$. The density functional theory is used within local density approximation. Total energy, chemical potential, addition energy spectra, and the shell structure are determined and the results obtained are compared for cases with and without impurity. It is observed that the capacitive energy with the impurity increases in the 1*s* shell with respect to the case without the impurity.

DOI: 10.1103/PhysRevB.72.125323 PACS number(s): 73.21.La, 73.23.Hk, 71.15.Mb

I. INTRODUCTION

The recent developments in the fabrication technology have given an opportunity to confine the electrons in two-, one-, and zero-dimensional semiconductor structures.[1,2] The zero-dimensional quantum dot (QD) is also called an artificial atom because it exhibits atomic properties. It is important to understand the electronic structure of QD for technological applications, such as single electron transistor, quantum dot infrared photodetector. Therefore, these are extensively studied in condensed matter physics both theoretically and experimentally.[3,4]

The number of electrons in the QD is very important for many physical properties of these structures, since with increasing number of electrons the electron-electron interaction becomes important. A number of studies have been performed on many-electron effects in semiconductor QDs.[3,5–10] An extensive review on electronic structure of QDs is reported by Reimann and Manninen.[10] Nowadays, powerful single-electron capacitance spectroscopy techniques,[3,11–13] infrared absorption,[14,15] and conductance measurements[11,12] have made available investigation of the discrete level structure, electron addition spectra, which is also known as capacitive energy, and many-body effects in electronic structure of single and coupled quantum dots. The Coulomb blockade effects are extensively studied for different physical conditions.[3,10,16] In device applications, especially for single-electron devices, the Coulomb blockade effect is very important.[3] This mechanism is used in quantum dot and/or tunnel junction systems to improve the current control in single-electron devices.[17]

The electronic properties of hydrogenic donor states, on the other hand, have also been studied widely as a function of dot radius, donor position, dielectric constant, temperature, etc.[18–21] for one and two electron QDs with an impurity which are called D^0 and D^- centers. The electronic structure of a many-electron two-dimensional QD with a hydrogenic impurity has been studied by Lee *et al.*[22] for a harmonic potential. They have investigated the spin-polarization changes, binding energies and capacitive energies as functions of impurity position and the number of electrons. DiVincenzo[23] and Kane[24] have proposed that the electronic structure of donors in a QD plays an important role in the quantum computation.

The many-body effects on impurity states in a different system are considered in Refs. 25 and 26.

Many different calculational techniques are used for determining electron-electron interaction effects on the electronic structure of many-electron quantum dots, such as matrix diagonalization, configuration interaction, Hartree approximation, and Hartree-Fock techniques.[27–29]

The hydrogenic impurity problem in a spherical QD is studied by many authors. These studies are limited only to impurities containing one or two electrons. Although, the electronic structure of a many-electron QD with the impurity for harmonic confinement was studied by Lee *et al.*,[22] the case of a many-electron spherical QD with a hydrogenic impurity is not investigated so far. The main goal of this paper is to investigate the electronic structure of a many-electron spherical QD in the presence of a hydrogenic impurity. For this purpose, density functional theory (DFT) has been used in the Kohn-Sham[30] scheme with local density approximation (LDA). The total energy, chemical potential, addition energy spectra, and shell structure are determined with and without the impurity. It is seen that the capacitive energy increases by presence of the impurity in the 1*s* shell especially. Although, the similar behavior has been reported for a two-dimensional QD in Ref. 22, this effect is reported for the first time in this study for a spherical QD.

This paper is organized as follows. In the next section, we present our model and the formulation of the problem. Results and discussion are presented in Sec. III. In the last section, a conclusion is given.

II. THE MODEL

In our model, we consider a spherically symmetric quantum dot with radius R_{dot} which is embedded in a bulk semiconductor. We use effective mass approximation and BenDaniel-Duke boundary conditions for the self-consistent calculations. In the effective mass approximation, for a spherically symmetric *N*-electron quantum dot with radius R_{dot} single-particle Kohn-Sham equation is given as

$$\left[-\frac{\hbar^2}{2}\vec{\nabla}_r\left(\frac{1}{m^*(r)}\vec{\nabla}_r\right)-\frac{Ze^2}{|\vec{r}-\vec{r}_i|}+\frac{\ell(\ell+1)\hbar}{2m^*(r)r^2}-e\Phi_{e-e}+V_b+V_{xc}\right]\varphi_i(r)=\varepsilon_i\varphi_i(r). \quad (1)$$

Here, m^* is the position-dependent electron's effective mass, Z is the charge of the impurity, ℓ is the angular momentum quantum number, $\Phi_{e\text{-}e}$ is the Hartree potential between electrons, V_b is the confining potential and V_{xc} is the exchange-correlation potential. The Hartree potential is determined from the Poisson equation,

$$\nabla^2\Phi_{e-e}=\frac{en_e(r)}{\kappa(r)}, \quad (2)$$

where $n_e(r)$ is the electron density and $\kappa(r)$ is the dielectric constant of the structure. The electron density is

$$n_e(r)=\frac{1}{4\pi}\sum_{\ell=0}^{p}2(2\ell+1)\sum_{n=1}^{np}|\varphi_{n,\ell}(r)|^2+\frac{1}{4\pi}q|\varphi_{nq,\ell q}(r)|^2, \quad (3)$$

where $2(2\ell+1)$ is the spin and magnetic degeneracies, p, and np are the angular momentum quantum number and principle quantum number of the fully occupied states, respectively, q is the number of remaining electrons in the last state, nq, and ℓq are the principle quantum number and angular momentum quantum number of the last state, respectively. We have employed Perdew and Zunger[32] expression for the exchange-correlation energy and potential which is the parametrization of the Monte Carlo result of Ceperley and Alder.[31]

In order to determine the single particle energy levels, Eqs. (1)–(3) are solved self-consistently in the local density approximation and then we calculate total energy of the system using

$$E=\sum_{i=1}^{N}\varepsilon_i-\frac{e}{2}\int\Phi_{e-e}n(r)d^3r+E_{xc}[n(r)]-\int V_{xc}[n(r)]n(r)d^3r. \quad (4)$$

We employ matrix diagonalization technique for the determination of single particle energies. For this purpose, the Hamiltonian operator is discretized on a uniform radial mesh in 1D using the finite differences, then Eq. (1) can be reduced to a matrix eigenvalue equation. Eigenvalues and eigenvectors of this matrix equation are determined by EISPACK subroutine. These eigenvectors are used in Eq. (3) for determining the charge density. The charge density in turn is used in exchange-correlation potential and Poisson equation, Eq. (2), and thus the Hartree potential $\Phi_{e\text{-}e}$ is calculated. The finite difference technique with Gauss elimination method is used for calculation of the Hartree potential. In order to perform a self-consistent calculation, Hartree and exchange-correlation potential are substituted into Eq. (1) and this process is continued until convergence is obtained.

We have calculated the self-consistent total energy $E(N)$ for the N-electron spherical QD. The chemical potential, $\mu(N)$, is the energy required to add an electron to the system having $(N-1)$ electron and is defined as total energy difference between the cases of N electrons and the $(N-1)$ electrons, namely,

$$\mu(N)=E(N)-E(N-1). \quad (5)$$

The capacitance of the QD can be derived from the chemical potential[33,34] as

$$C(N)=\frac{e^2}{\mu(N+1)-\mu(N)}. \quad (6)$$

The capacitive or addition energy, $\Delta A(N)=e^2/C(N)$, for the N-electron system is defined as

$$\Delta A(N)=\mu(N+1)-\mu(N)=E(N+1)+E(N-1)-2E(N). \quad (7)$$

The capacitive energy in the DFT is equal to the energy gap between the lowest unoccupied and highest occupied states for an N-electron QD.[33]

III. RESULTS AND DISCUSSION

Following theoretical studies on spherical quantum dots, we use the material parameters of GaAs for the well region and that of AlGaAs for the barrier region,[19,35,36] because their basic physical properties such as band mismatch, effective masses, and dielectric constants are better known.[37] The parameters of more realistic structures can easily be used in the present calculation.

We have used atomic units throughout our calculations. Effective Bohr radius is $a_0^*=100$ Å and effective Rydberg energy is $R_y^*=5.5$ meV. We take $m_{\mathrm{GaAs}}=0.067m_0$, $m_{\mathrm{AlGaAs}}=0.092m_0$, $V_b=228$ meV, $\kappa_{\mathrm{GaAs}}=13.1$, $\kappa_{\mathrm{AlGaAs}}=12.2$ as material parameters. We denote the effective masses of electrons inside GaAs and AlGaAs as m_1^* and m_2^*, and similarly the dielectric constants as κ_1 and κ_2, respectively. The position-dependent effective mass and the dielectric constant may be defined as follows:[19]

$$m^*(r)=\begin{cases}1, & r<R_{\mathrm{dot}},\\ \dfrac{m_2^*}{m_1^*}, & r>R_{\mathrm{dot}},\end{cases}$$

$$\kappa(r)=\begin{cases}1, & r<R_{\mathrm{dot}},\\ \dfrac{\kappa_2}{\kappa_1}, & r>R_{\mathrm{dot}}.\end{cases} \quad (8)$$

Figure 1 shows an effective potential $\{(-Ze^2/r)+[\ell(\ell+1)\hbar^2/2mr^2]\}$ including the effects of both the Coulomb potential due to impurity and the angular momentum. As seen from the figure, while the potential for $\ell=0$ is attractive, it is repulsive for $\ell>0$ at the center of the QD. The influence of the repulsive potential decreases with the impurity in comparison to the case without the impurity. The Coulomb potential has a singularity at $r=0$. In order to avoid the numeri-

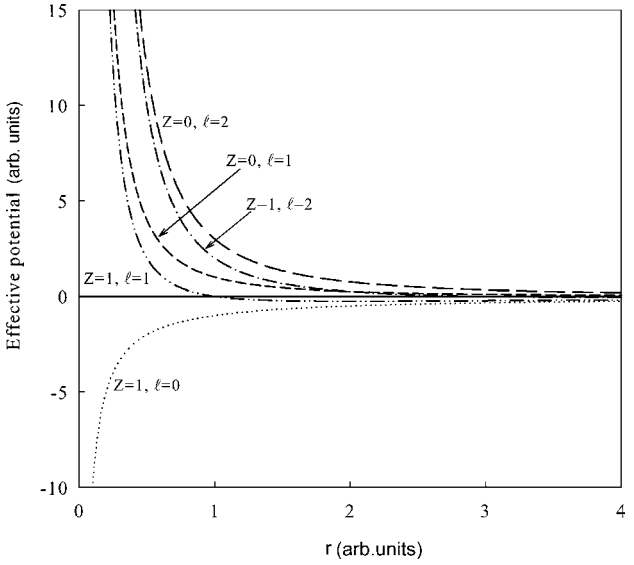

FIG. 1. Effective potential for different ℓ and Z values.

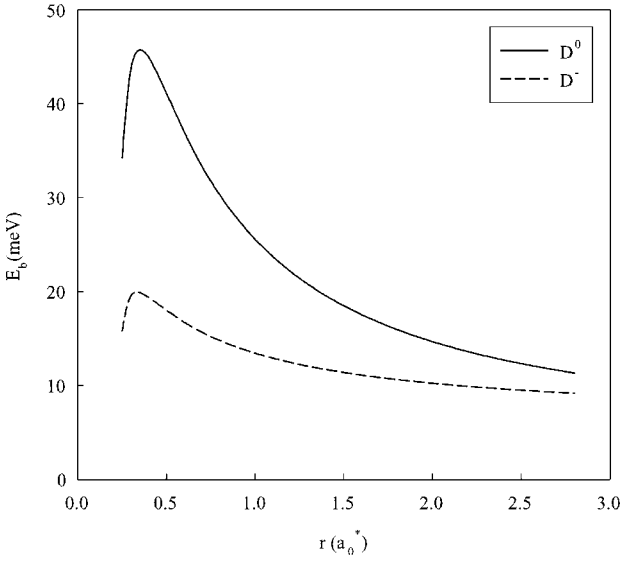

FIG. 2. Binding energy of D^0 and D^- center.

cal singularity of the impurity potential at the origin we use the cusp condition,[38] which modifies the eigenfunction as to take into account the effect of the singularity.

If the radius of the dot with a hydrogenic impurity is large enough, one electron in the dot is bound to this hydrogenic impurity to create a neutral entity (D^0).[35,36] A second electron also can bind to this single impurity as a result of polarization if the radius becomes larger. In this case, the structure is called a D^- center.[20,21,39] The binding energy of a neutral donor impurity is the difference between the total energies with and without impurity,[35,36] namely,

$$E_b(D^0) = E_0 - E(D^0). \tag{9}$$

Here, E_0 is the ground state of single electron without impurity in the QD and $E(D^0)$ is the lowest level of neutral donor. The binding energy of a D^- center is defined as

$$E_b(D^-) = E_0 + E(D^0) - E(D^-), \tag{10}$$

where $E(D^-)$ is the lowest level of D^- center.[21,39] Figure 2 shows the variation of the binding energy of D^0 and D^- center as a function of the dot radius.

The results are in a good agreement with previous studies.[36,40] Although it is not possible to bind more than two electrons to a single impurity, this impurity affects the electronic structure of the many-electron QD. It should be also noted that, if the charge of impurity in the QD increases ($Z=2,3\ldots$), the number of electrons binding to the impurity increases.

In Fig. 3, the variation of differences between total energies with and without impurity per electron with the dot radius is seen for various electron numbers. In this figure, the variation at $N=1$ is equal to binding energy of D^0 seen in the preceding figure. As seen from the figure, these differences between total energies per electron decrease while the number of electrons increase. This result shows that the influence of impurity is weaker at higher energy levels as the electron numbers increase.

The chemical potential, which is calculated by Eq. (5), is plotted in Figs. 4(a) and 4(b) for $Z=0$ and $Z=1$, respectively. Three groups have been observed in both figures. These groups correspond to three different orbitals, $1s$, $1p$, and $1d$. This is the well-known shell structure of a spherical quantum dot for bound states. The chemical potentials drop as the dot radius increases in both cases. As seen from Fig. 4(a), the chemical potential goes to zero when the dot radius becomes large especially for the $1s$ orbital. The total energy goes to zero for the ground state as the dot radius is increased. This total energy approaches the binding energy, which is negative for the large dot radius, and $Z=1$. Consequently, the chemical potential gains a negative value in the $1s$ orbital.

Figure 5 shows the variation of the capacitive energy with the number of electrons for $Z=0$ and $Z=1$ at $R_{\mathrm{dot}}=1.4a_0^*$. The result presented is for $R_{\mathrm{dot}}=1.4a_0^*$ since 18 electrons can be

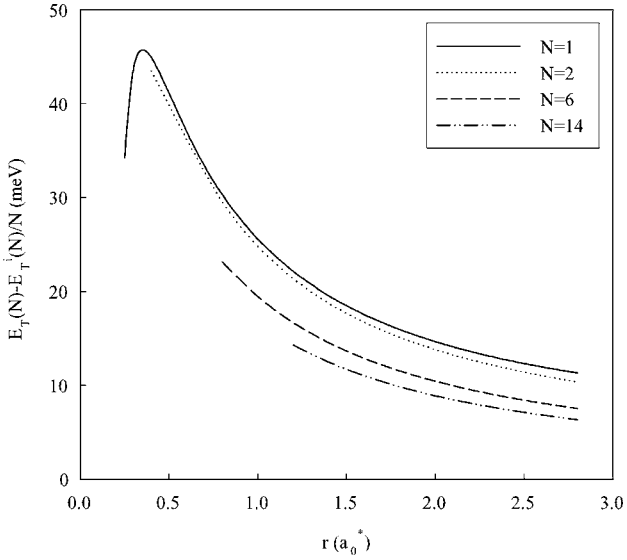

FIG. 3. Difference between the total energies per an electron with and without the impurity.

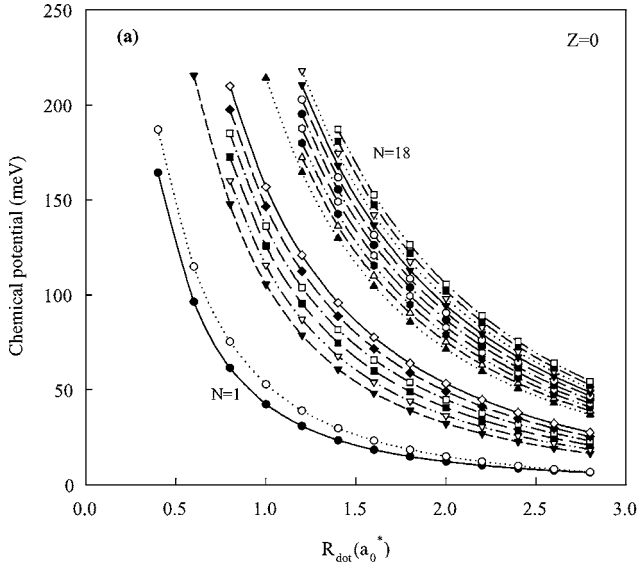

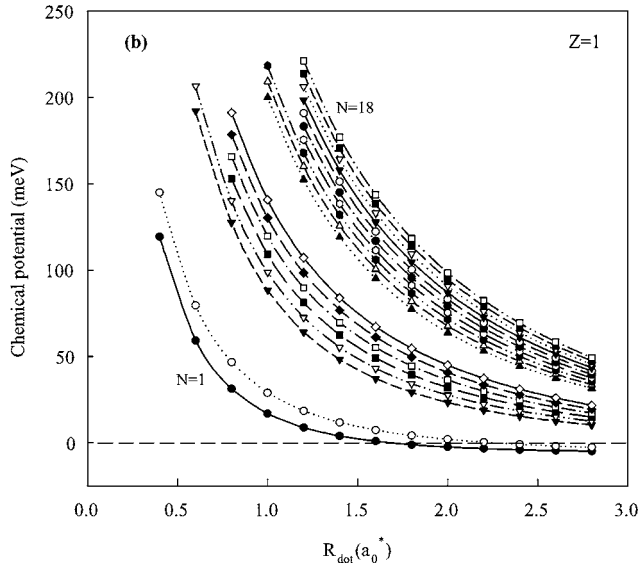

FIG. 4. Variation of the chemical potential with the dot radius (a) for $Z=0$, (b) for $Z=1$.

confined at this dot radius. However, similar trend is also obtained for the other dot radii. The peaks are observed when the shells are fully occupied and the numbers corresponding to these peaks are called magic numbers. The addition or capacitive energy is very high at the magic numbers for both $Z=0$ and $Z=1$ cases, due to the fully occupied shells. This reflects the fact that the addition of one electron to the system is very difficult at these magic numbers. But, it is very easy for open shells.

Another important result seen from the figure is that the addition energy is greater for the $Z=1$ than for the $Z=0$ case. This is an unexpected result. The expected result is that the addition energy is lower at the $Z=1$ than for the $Z=0$ case because of the attractive Coulomb potential of the impurity at the $1s$ orbital. Similar result is found for eight electrons at the $1p$ orbital but it is not very dominant. In other words, when the number of electrons increases, the effect of the impurity decreases. The electron distribution function is useful to explain these results. The distribution function of electron gas with and without impurity is seen in Fig. 6 for $N=2$ and $R=1.4a_0^*$. It is seen that the distribution function shows a uniform broadening at the absence of the impurity, $Z=0$. In this case, distance between electrons is large and the repulsive Coulomb potential is relatively small. Hence, the addition of second electrons to the QD is relatively easier. Although similar distribution is observed at the inclusion of the impurity, $Z=1$, it shifts towards to quantum dot center. Consequently, distance between electrons is smaller and the repulsive Coulomb potential becomes more effective. Therefore, addition of a second electron requires more energy than the $Z=0$ case.

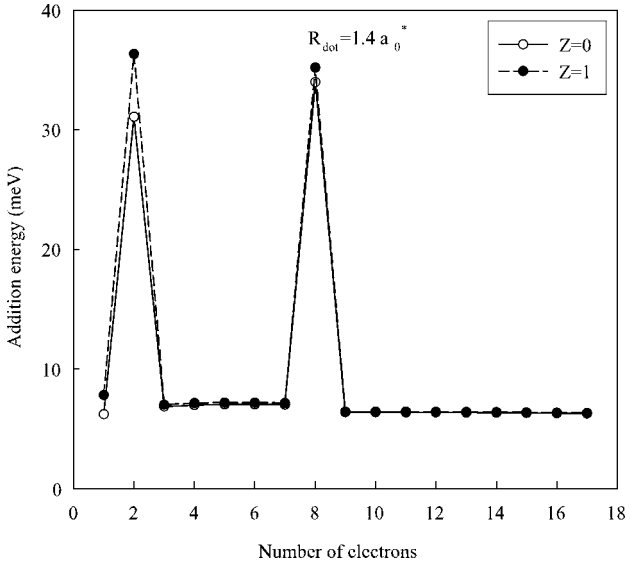

FIG. 5. Variation of capacitive energy with number of electrons for the $Z=0$ and $Z=1$ cases.

Figure 7 is the same as Fig. 6 except that the number of electrons is 8. As seen from the figure, the electron distribu-

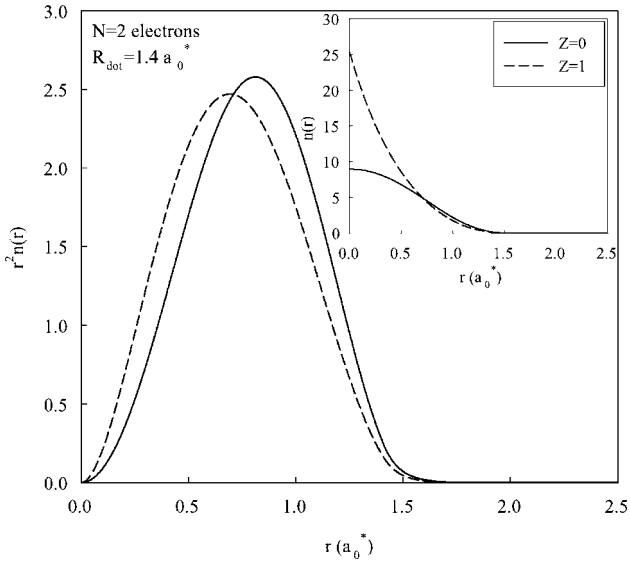

FIG. 6. Electron density probability distribution for the $N=2$, $Z=0$, and $Z=1$ cases. The inset shows the density distribution without the r^2 factor.

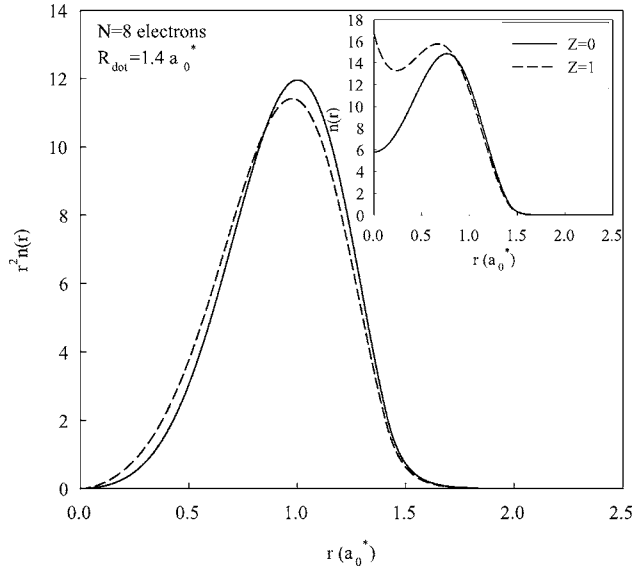

FIG. 7. Same as Fig. 6 but for $N=8$.

tion functions are very similar for $Z=0$ and $Z=1$ cases. Increasing the number of electrons in the QD increases the screening of the impurity and decreases the attractive properties of the Coulomb potential due to the impurity. Hence, the energy required for addition of the eighth electron to the QD is approximately equal, with and without the impurity as seen in Fig. 5.

Even though the addition energy is enhanced by the hydrogenic impurity, the electron numbers confined in the QD go up in the presence of the impurity. This case is demonstrated in Fig. 8. As seen from the figure, only one electron can be confined for $R_{\mathrm{dot}}=0.25a_0^*$ and 18 electrons confined for $R_{\mathrm{dot}}=1.4a_0^*$ at the $Z=0$ case. Nevertheless, two electrons can be confined at $R_{\mathrm{dot}}=0.25a_0^*$ and 18 electrons confined for $R_{\mathrm{dot}}=1.2a_0^*$ at $Z=1$ case.

In Fig. 9, we plot the variation of the capacitive energy with the dot radii for $N=2$ and 8 electrons and $Z=0$ and $Z=1$ cases. The difference between the capacitive energies

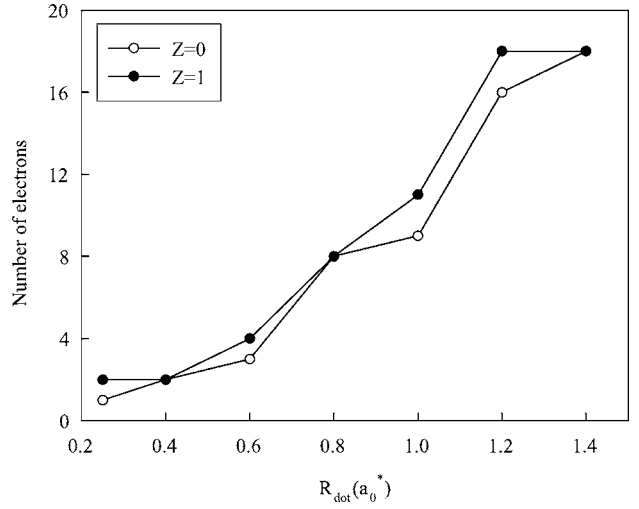

FIG. 8. Confinement electron numbers in QD with different dot radii for $Z=0$ and $Z=1$ cases.

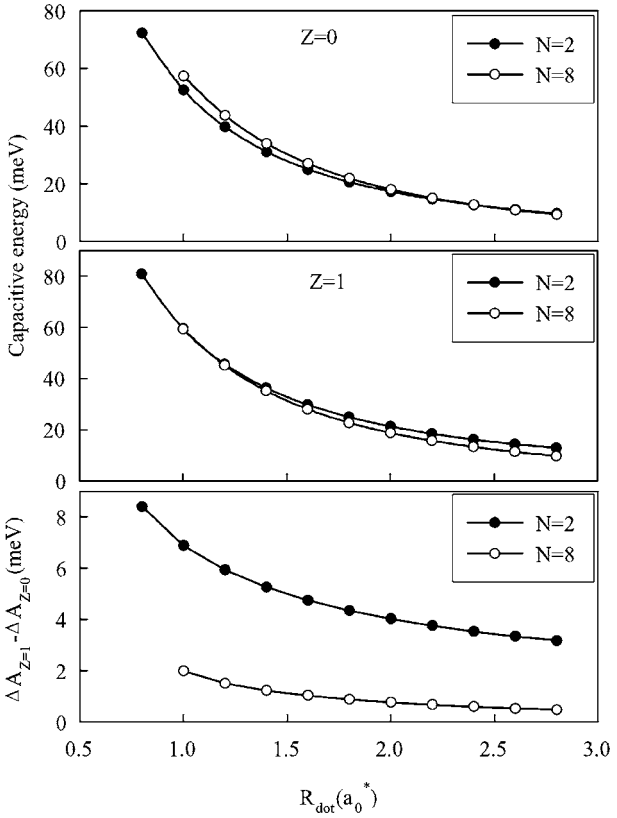

FIG. 9. The capacitive energies as a function of the dot radius (a) for $Z=0$ and (b) for $Z=1$. (c) shows the difference of the addition energies between (b) and (a).

with and without the impurity for the same electron numbers is shown in this figure. As seen from Fig. 9(a), the capacitive energies drop as the dot radius increases. In addition, the capacitive energy for $N=2$ is lower than for $N=8$ in the $Z=0$ case at small dot radii and it becomes equal for $N=2$ and 8 at larger dot radii. However, as seen in Fig. 9(b), while the capacitive energies are equal for $N=2$ and 8 at small dot radii, it becomes lower for $N=8$ than for $N=2$ at larger dot radii in the $Z=1$ case. As seen, the impurity inverts the character of capacitive energy structure of spherical QD at the $Z=0$ case. Figure 9(c) shows the difference between the addition energies with and without the impurity. As seen from the figure, the impurity effect is more apparent at s shell, $N=2$ case and at small dot radii for $N=2$ and 8 and this effect decreases while the dot radius increases for both electron numbers. Furthermore, influence of the impurity goes to zero for $N=8$ at large dot radii.

IV. CONCLUSION

We have calculated the electronic structure of a many-electron spherical quantum dot as a function of the number of electrons and dot radius with and without the impurity. Here, the electron numbers have been taken as maximum 18. We have used density functional theory within local density approximation to take into account the many-body effects. Although only two electrons bind to impurity, it is seen that the impurity affects the electronic structure of a many-

electron QD. These effects are considerable on the physical quantity corresponds to the 1*s* orbital such as chemical potentials, capacitive energies, density distributions, etc. We do not observe any change in the shell structure of the QD with the introduction of an impurity. The surprising effect of impurity is observed at the addition energy of the second electron. As the energy required is much more for adding a second electron to QD for the $Z=1$ case, this energy is much less for the $Z=0$ case. This property can be used for designing devices. Also, important changes in the electronic properties of a many-electron quantum dot can be made by increasing the charge of the impurity (helium like $Z=2$, lithium like $Z=3$, etc.) and these changes may be very useful and important for various device applications.

ACKNOWLEDGMENT

This work was partially supported by Selçuk University under Grant No. BAP2001/112.

*Electronic address: sahinm@selcuk.edu.tr

[1] L. Banyai and S. W. Koch, *Semiconductor Quantum Dots* (World Scientific, Singapore, 1993).
[2] D. Bimberg, M. Grundmann, and N. N. Ledentsov, *Quantum Dot Heterostructures* (Wiley, Chichester, 1999).
[3] L. P. Kouwenhoven, D. G. Austing, and S. Tarucha, Rep. Prog. Phys. **64**, 701 (2001).
[4] S. Bednarek, B. Szafran, and J. Adamowski, Phys. Rev. B **61**, 4461 (2000).
[5] I.-H. Lee, V. Rao, R. M. Martin, and J. P. Leburton, Phys. Rev. B **57**, 9035 (1998).
[6] L. R. C. Fonseca, J. L. Jimenez, J. P. Leburton, and R. M. Martin, Phys. Rev. B **57**, 4017 (1998).
[7] R. K. Pandey, M. K. Harbola, V. Ranjan, and V. A. Singh, Bull. Mater. Sci. **26**, 63 (2003).
[8] I.-H. Lee, J. Korean Phys. Soc. **34**, S46 (1999).
[9] S. Akbar and I.-H. Lee, Phys. Rev. B **63**, 165301 (2001).
[10] S. M. Reimann and M. Manninen, Rev. Mod. Phys. **74**, 1283 (2002).
[11] R. C. Ashoori, H. L. Stormer, J. S. Weiner, L. N. Pfeiffer, K. W. Baldwin, and K. W. West, Phys. Rev. Lett. **71**, 613 (1993).
[12] J. Weis, R. J. Haug, K. v. Klitzing, and K. Ploog, Phys. Rev. Lett. **71**, 4019 (1993).
[13] S. Tarucha, D. G. Austing, T. Honda, R. J. van der Hage, and L. P. Kouwenhoven, Phys. Rev. Lett. **77**, 3613 (1996).
[14] A. Lorke, J. P. Kotthaus, and K. Ploog, Phys. Rev. Lett. **64**, 2559 (1990).
[15] T. Demel, D. Heitmann, P. Grambow, and K. Ploog, Phys. Rev. Lett. **64**, 788 (1990).
[16] J. See, P. Dollfus, S. Galdin, and P. Hesto, Physica E (Amsterdam) **21**, 496 (2004).
[17] H. Grabert and M. H. Devoret, *Single Charge Tunneling: Coulomb Blockade Phenomena in Nanostructures*, Series B: Physics, Vol. 294 (Plenum, New York, 1992).
[18] A. M. Elabsy, Phys. Scr. **59**, 328 (1999).
[19] R. Buczko and F. Bassani, Phys. Rev. B **54**, 2667 (1996).
[20] D. Chandramohan, S. Balasubramanian, and M. Tomak, Phys. Rev. B **37**, 7102 (1988).
[21] J.-L. Zhu, J.-H. Zhao, W.-H. Duan, and B.-L. Gu, Phys. Rev. B **46**, 7546 (1992).
[22] I.-H. Lee, K.-H. Ahn, Y.-H. Kim, R. M. Martin, and J.-P. Leburton, Phys. Rev. B **60**, 13720 (1999).
[23] D. P. DiVincenzo, Nature (London) **393**, 113 (1998).
[24] B. E. Kane, Nature (London) **393**, 133 (1998).
[25] V. Gudmundsson, *Spectroscodpy of Semiconductor Microstructures*, NATO-ASI Series B206, Vol. 517 (Plenum, New York, 1989).
[26] V. Gudmundsson, Solid State Commun. **74**, 63 (1990).
[27] J. Gu and J. Q. Liang, Phys. Lett. A **323**, 132 (2004).
[28] B. Reusch and H. Grabert, Phys. Rev. B **68**, 045309 (2003).
[29] S. Bednarek, B. Szafran, and J. Adamowski, Phys. Rev. B **59**, 13036 (1999).
[30] W. Kohn and L. J. Sham, Phys. Rev. **140**, A1133 (1965).
[31] D. M. Ceperley and B. J. Alder, Phys. Rev. Lett. **45**, 566 (1980).
[32] J. P. Perdew and A. Zunger, Phys. Rev. B **23**, 5048 (1981).
[33] G. J. Iafrate, K. Hess, J. B. Krieger, and M. Macucci, Phys. Rev. B **52**, 10737 (1995).
[34] M. A. Kastner, Phys. Today **46**, 24 (1993).
[35] J.-L. Zhu, J.-J. Xiong, and B.-L. Gu, Phys. Rev. B **41**, 6001 (1990).
[36] N. Porras-Montenegro and S. T. Pérez-Merchancano, Phys. Rev. B **46**, 9780 (1992).
[37] S. Adachi, J. Appl. Phys. **58**, R1 (1985).
[38] J. M. Thijssen, *Computational Physics* (Cambridge University Press, Cambridge, 1999).
[39] B. Szafran, J. Adamowski, and B. Stebe, J. Phys.: Condens. Matter **10**, 7575 (1998).
[40] Z.-Y. Deng, J.-K. Gou, and T.-R. Lai, J. Phys.: Condens. Matter **6**, 5949 (1994).